The changes in silyl radical electron affinities and silane acidities with methyl substitution reveal a modest destabilization effect. Methyl groups lower the electron affinities of the radicals and decrease the acidities of the silanes, evidence for destabilization of the silyl anion. Phenyl does not show such destabilization.

Experimental results and theoretical investigations involving neutral organosilanes are pertinent to understanding the interactions involved in the observed methyl destabilization of silyl anions. Michl and co-workers,[42] in an investigation of electronic perturbations caused by substituents on benzene, such as $-SiH_3$, $-SiH_2Me$, $-SiHMe_2$, and $SiMe_3$, using magnetic circular dichroism (MCD) spectroscopy, found evidence for π-electron donation from methyl to silicon. The π-acceptor ability of a SiH_3 substituent was observed to decrease with successive replacements of Me for H. These MCD experimental results were rationalized within the framework of perturbational molecular orbital theory: the filled, π-type bonding orbitals of the methyl group donate electron density to the unfilled, π-type antibonding orbitals of silicon. Another way to describe the interaction is back-bonding from the C-H bonding orbitals of the methyl group to the Si-H or Si-C antibonding orbitals. This results, in part, from the electropositive nature of silicon which causes the bonding Si-R(H) orbitals to have large coefficients on R(H) and the antibonding orbitals to have large coefficients on Si.

Calculations indicate this net $C_\pi \rightarrow Si_\pi^*$ electron donation is important in silaethane[43] and also occurs in methyl silyl anion.[40,44,45] In the silyl anion, however, where the excess charge resides predominantly on the silicon atom, this net electron-donating interaction is destabilizing. With respect to the radical, the relative stabilities of SiH_3^-, $MeSiH_3^-$, and Me_3SiH^- and those of $PhSiH_2^-$ and $PhMeSiH^-$ are consistent with this description. The effect of methyl substitution on the anion stability is not additive, but appears to show saturation.

The photodetachment spectra give evidence for low-lying (ca. 2 eV) valence electronic states in trimethylsilyl anion. The rapid increase in the cross sections of the other anions suggests that they also have low-lying electronic states, although the maxima are beyond the range of our data. The effect of methyl groups in raising the orbital energy of the nonbonding electrons appears here also, with trimethylsilyl anion having its transition at an energy lower than the corresponding one in the other anions. The excited state very likely involves a Si-R antibonding orbital. This orbital is expected to have a large contribution (large coefficient) on silicon.

Conclusions

We have measured gas-phase equilibrium constants and electron photodetachment onsets for a series of alkyl- and aryl-substituted silyl compounds and report the resultant acidities, electron affinities, and bond dissociation energies. The data indicate that (1) silyl anions are quite stable, (2) methyl groups cause modest destabilization in organosilyl anions, (3) resonance delocalization appears to be unimportant in stabilizing silyl anions, and (4) substitution and geometry changes in organosilyl anions and radicals are relatively unimportant.[46]

Acknowledgment. We are grateful for support by the National Science Foundation, and materials made available by the San Francisco Laser Center, supported by the National Science Foundation. We thank Professors J. Michl, G. B. Ellison, and R. Damrauer for helpful discussions.

Registry No. Me_3SiH, 993-07-7; $MeSiH_3$, 992-94-9; $PhMeSiH_2$, 766-08-5; SiH_4, 7803-62-5; $PhSiH_3$, 694-53-1; $Me_3Si^\bullet$, 16571-41-8; $MeSiH_2^\bullet$, 51220-22-5; $PhMeSiH^\bullet$, 119946-89-3; $SiH_3^\bullet$, 13765-44-1; $PhSiH_2^\bullet$, 72975-30-5.

(42) Weeks, G. H.; Adcock, W.; Klingensmith, K. A.; Waluk, J. W.; West, R.; Vasak, M.; Downing, J.; Michl, J. *Pure Appl. Chem.* **1986**, *58*, 39.
(43) Bernardi, F.; Bottoni, A.; Tonachini, G. *Theor. Chim. Acta* **1979**, *52*, 37.
(44) Hopkinson, A. C.; Lien, M. H. *Tetrahedron* **1981**, *37*, 1105.
(45) For an experimental determination of the stabilization of carbanions by α-silyl groups, see ref 25.
(46) **Added in Proof**: See Gordon, Boatz, and Walsh (Gordon, M. S.; Boatz; Walsh, R. *J. Phys. Chem.* **1989**, *93*, 1484) for a discussion of additivity in silane heats of formation.

Reactions of Methanol Clusters following Multiphoton Ionization

S. Morgan, R. G. Keesee, and A. W. Castleman, Jr.*

Contribution from the Department of Chemistry, The Pennsylvania State University, University Park, Pennsylvania 16802. *Received June 3, 1988*

Abstract: Clusters of methanol formed in a supersonic expansion are subjected to multiphoton ionization (MPI) at 266 nm using a pulsed Nd:YAG laser. The resulting cluster ions, $H^+(CH_3OH)_n$, are found to undergo several intracluster reaction pathways which display a dependence on the degree of aggregation. In addition to the evaporation loss of methanol monomers at all sizes, and the loss of H_2O from the protonated dimer, it is found that a channel corresponding to $(CH_3)_2O$ and CH_3OH loss, with H_2O retention, also occurs. For clusters comprised of four to nine methanol molecules, the $(CH_3)_2O$ elimination is observed to take place over the time window of about 1 to 15 μs after ionization, while prompt $(CH_3)_2O$ elimination also occurs in the size range above $n = 7$. The mechanisms are considered in terms of estimated energetics for the various pathways.

Under certain conditions following the ionization of a cluster, reactions proceed between various moieties within the cluster ion that in terms of products often parallel bimolecular gas-phase ion-molecule reactions. Several examples have been reported in the literature for systems comprised of both hydrogen-bonded clusters as well as ones stabilized by weaker van der Waals dispersion forces.[1-4]

Clusters comprised of methanol molecules represent a promising system for exploring reactions as a function of cluster size. Reactions between methanol ions and methanol have been well explored in the gas phase by both ICR[5] and fast-flow reactor

(1) Klots, C. E.; Compton, R. N. *J. Chem. Phys.* **1978**, *69*, 1644.
(2) Echt, O.; Dao, P. D.; Morgan, S.; Castleman, A. W., Jr. *J. Chem. Phys.* **1985**, *82*, 4076.
(3) Garvey, J. F.; Bernstein, R. B. *J. Am. Chem. Soc.* **1987**, *109*, 1921.
(4) Stephan, K.; Futrell, J. H.; Peterson, K. I.; Castleman, A. W., Jr.; Mark, T. D. *J. Chem. Phys.* **1982**, *77*, 2408.

0002-7863/89/1511-3841$01.50/0

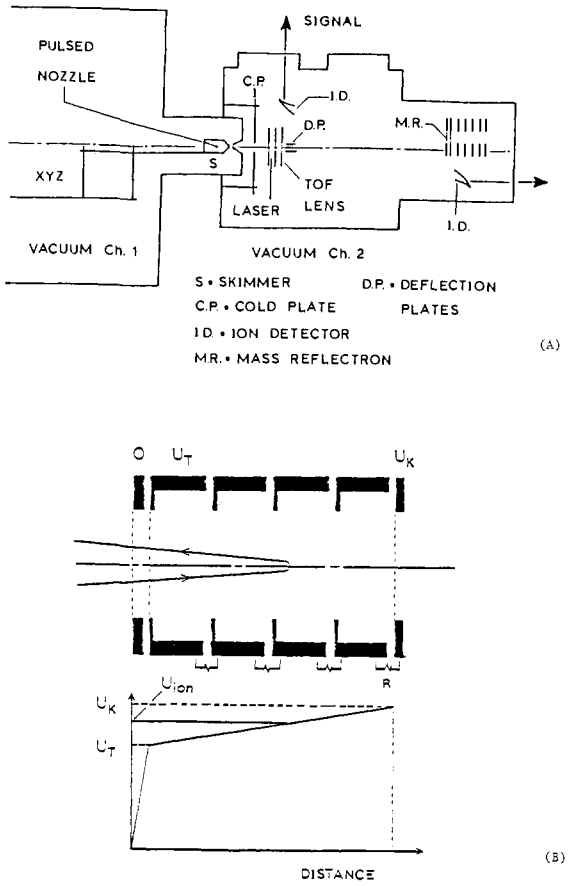

Figure 1. (A) Schematic diagram of the time-of-flight mass spectrometer including the reflectron. (B) Trajectory of an ion with energy corresponding to U_{ion} where U_T and U_K are the potentials on grids T and K of the reflection.

techniques.[6] Alcohol ions are known to undergo a number of isomerization and dehydration reactions leading to dimethyl ether and water, and it is interesting to compare results of gas-phase experiments and known thermochemistry of protonated systems comprised of alcohol–water mixtures[7,8] with reactions which occur in clusters.

In an earlier study,[9] we investigated internal ion–molecule reactions in small methanol clusters and observed that the protonated methanol dimer underwent a delayed reaction corresponding to the production of protonated dimethyl ether and the loss of an H_2O molecule. No similar reaction channel was found for neighboring cluster sizes, a finding which was in accord with gas-phase ion–molecule reaction studies.[5] The present paper represents an extension of the earlier study to clusters of larger size. Additional reaction channels which display a specificity with the degree of aggregation are reported herein.

Experimental Section

The apparatus used in these studies has been described in detail elsewhere.[2] Hence only a brief description of the features pertinent to the present study are given. Neutral methanol clusters are produced in an argon-seeded supersonic expansion of methanol vapor into vacuum from a pulsed valve source. The cluster beam is subjected to multiphoton ionization, and the resulting cluster ions are analyzed in a time-of-flight (TOF) mass spectrometer equipped with a reflecting electric field (reflectron). The molecular beam is intersected by a laser beam of fixed wavelength (266 nm), provided by frequency doubling the second harmonic of a Nd:YAG laser. Typical photon fluxes of 10^{16} photons per pulse of approximately 6-ns duration are obtained. Ions formed by multiphoton absorption are accelerated in a series of two electrostatic fields to approximately 2 keV, deflected by a few degrees in a transverse field to separate the ion and neutral beams, and subsequently detected by a particle multiplier (CEM 4700). The time-resolved ion current representing the TOF mass spectrum is digitized and signal averaged by a transient recorder (Gould Biomation 4500) with 10-ns resolution.

In conventional TOF mass spectrometry (without a reflectron), dissociation products born in the field-free flight region appear at parent ion masses such that the processes leading to their formation cannot be directly studied. Incorporation of a reflection at the end of the flight tube of the TOF MS enables investigation of dissociation processes. Upon application of appropriate potentials at the reflection grids, daughter ions born in the field-free region and undissociated parent ions are temporally separated, thus enabling their separate detection. Unique identification of the initial and final mass of an ion is made on the basis of both time differences and energy analysis as discussed previously.[2]

A schematic of the reflectron, shown in Figure 1, displays the nature of the reflecting fields which enable separation of daughter and parent ions. The utility of energy analysis is also evident in Figure 1B. Parent ion intensity can be completely eliminated from the mass spectrum by reducing the potential at U_K to a value that allows the parent ions to penetrate through the reflectron. Successive changes of potential enable separation of daughter ions of various kinetic energies.

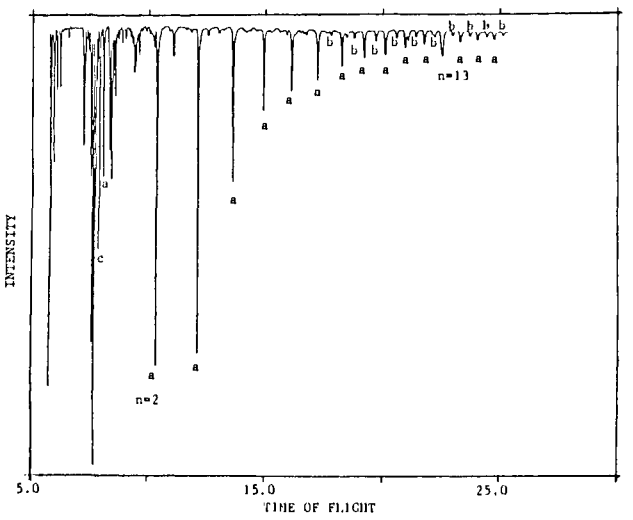

Figure 2. TOF spectrum of $H^+(CH_3OH)_n$ at 266 nm (time in μs).

Results and Discussion

Conventional Mass Spectrum. Experiments were conducted by expanding an approximately 10–15% mixture of methanol in argon at pressures ranging from a few hundred to a thousand Torr. A conventional time-of-flight mass spectrum (no reflectron) recorded by using the channeltron electron multiplier on the axis of the detection chamber is displayed in Figure 2. The figure shows typical results from the expansion of a 1:7 mixture of methanol vapor and argon at 450 Torr backing pressure. The laser power at 266 nm is 16 mJ/pulse with a tightly focused beam resulting in a laser fluence of about 10^9 W/cm^2. The averaged spectrum is accumulated over 2560 laser shots.

Two distinct distributions of cluster ions are observed in Figure 2 along with other ions of interest. The sequence of ions labeled **a** consists of protonated methanol clusters of form $H^+(CH_3OH)_n$. A second sequence labeled **b** is clearly evident after the $n = 7$ peak in the **a** series; these ions are of form $H^+(H_2O)(CH_3OH)_n$. A peak corresponding in stoichiometry to CH_3O^+ (ionization potential 11.55 eV from CH_3OH), labeled **c**, is also observed and apparently arises from 3-photon nonresonant ionization of CH_3OH at 266 nm. The undissociated monomer ion, CH_3OH^+, is not observed in the mass spectrum. No intensity anomalies are observed in the smooth distribution of protonated methanol cluster ions. The prominence at $n = 13$ and the shoulder on the right of $n = 11$ result from contributions of background peaks. The absence of intensity anomalies, frequently referred to as magic

(5) (a) Bowers, M. T.; Su, T.; Anicich, V. G. *J. Chem. Phys.* **1973**, *58*, 5175. (b) Bass, L. M.; Cates, R. D.; Jarrold, M. F.; Kirchner, N. J.; Bowers, M. T. *J. Am. Chem. Soc.* **1983**, *105*, 7024.
(6) Graul, S. T.; Squires, R. R. *Int. J. Mass. Spectrom. Ion Proc.* **1987**, *81*, 183.
(7) Morton, T. H. *Tetrahedron* **1982**, *38*, 3195.
(8) Keesee, R. G.; Castleman, A. W., Jr. *J. Phys. Chem. Ref. Data* **1986**, *15*, 1011.
(9) Morgan, S.; Castleman, A. W., Jr. *J. Am. Chem. Soc.* **1987**, *109*, 2867.

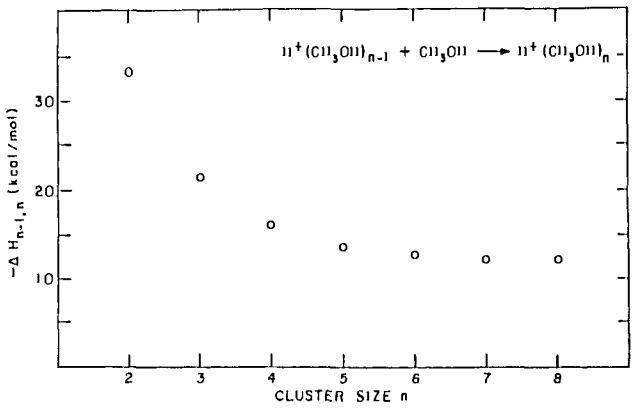

Figure 3. Enthalpies, $-\Delta H_{n-1,n}$, for successive additions of CH_3OH onto $H^+(CH_3OH)$ plotted versus number of ligands n (data from ref 10).

numbers, is not surprising in light of thermodynamic measurements. Figure 3, a plot of enthalpy of association (at 298 K) for successive addition of methanol moieties onto $H^+(CH_3OH)$ versus cluster size, is based on published thermodynamic results[10] derived from high-pressure mass spectrometric measurements. A smoothly decreasing trend in enthalpy change with no abrupt breaks is indicated up to $n = 8$; therefore, from thermodynamic considerations, intensity anomalies are not expected.[11,12]

The origin of the sequence **a**, corresponding to protonated methanol peaks, is the rapid intracluster proton-transfer reaction following ionization of the neutral clusters as shown below. This reaction has a well-known bimolecular counterpart that proceeds at near collision rate.[5]

$$(CH_3OH)_n^+ \rightarrow H^+(CH_3OH)_{n-1} + CH_3O \qquad (1)$$

Two mechanisms for the formation of sequence **b**, $H^+(H_2O)(CH_3OH)_n$, are envisioned. Mechanism I involves an intracluster reaction between two methanol moieties, resulting in elimination of C_2H_6O. Methanol monomer may also be lost concurrently.

$$[H^+(CH_3OH)_n]^* \rightarrow H^+(H_2O)(CH_3OH)_{n-3} + (CH_3)_2O + CH_3OH \qquad (2)$$

Mechanism II requires the presence of mixed methanol–water neutral clusters resulting from the clustering of water impurities in the expansion mixture.

$$(H_2O)(CH_3OH)_n \xrightarrow{h\nu} H^+(H_2O)(CH_3OH)_{n-1} + CH_3O + e^- \qquad (3)$$

Mechanism I is considered much more likely for several reasons. Water is not an added component of the expansion mixture; it is therefore present only in trace amounts. Methanol used in the expansion mixtures contains 0.05% water impurity, and unopened new bottles are used to prepare each new mixture. Stace and Shukla[13] have studied cluster distributions resulting from the expansion of 1% methanol in water. Their results show that under such conditions the 1:1 CH_3OH:H_2O mixed cluster is of highest intensity followed by decreasing intensity for the 1:2, 1:3, and successive clusters; the trace constituent is present in diminishing amounts in higher order clusters comprised of the major component of the system. Therefore, a few percent H_2O in methanol expansion would be expected to yield cluster distributions which exhibit similar intensity characteristics with the highest intensity resulting from the 1:1 H_2O–CH_3OH cluster and successively decreasing intensities for higher methanol aggregate mixed species.

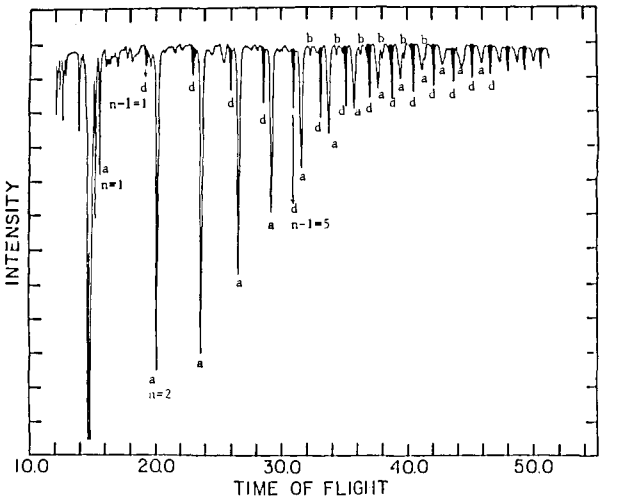

Figure 4. TOF spectrum of reflected ions at 266 nm (time in μs).

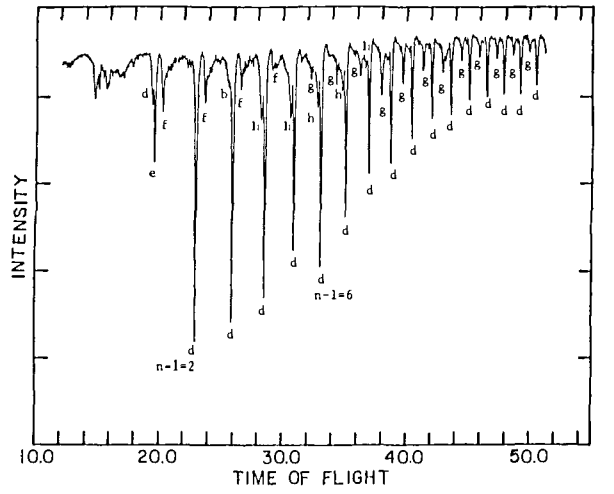

Figure 5. TOF spectrum of reflected daughter ions at 266 nm (time in μs).

Similar observations have been reported by others[13,14] for systems comprised of water with both methanol and ethanol.

The intensity distribution obtained in the present work and shown in Figure 2 is quite different from the one which would be expected based on the foregoing considerations; the maximum mixed cluster intensity occurs for the cluster of nine methanol moieties with one water. Additionally, the mixed cluster sequence is not even observed in the mass spectrum before the $n = 7$ peak. The dissimilarity of these two intensity patterns strongly indicates that the mixed clusters, $H^+(H_2O)(CH_3OH)_n$, do not arise from a neutral beam species. Additional evidence favoring the first mechanism is presented in the next section.

Reflection Mass Spectra. Incorporation of a reflectron in the TOF MS enables investigation of dissociation processes of methanol ion clusters by producing a time difference between undissociated parent ions and their daughter ions that are formed in the field-free region. A TOF spectrum of reflected ions, generated by multiphoton absorption at $\lambda = 266$ nm, is shown in Figure 4. In this experiment the stagnation pressure, P_0, is 550 Torr, the parent ion birth potential is 1164 V, and the spectrum is accumulated over 2560 laser shots. The spectrum exhibits two prominent peak sequences; the sequence labeled **a** represents parent ions of form $H^+(CH_3OH)_n$ and the **d**-labeled sequence (shaded) represents their daughter ions born in the drift region of form $H^+(CH_3OH)_{n-1}$. The potentials at the reflectron grids are $U_T = 0.997U_0$ and $U_K = 1.98U_0$; under such conditions, all daughter ions with a mass loss $m_p - m_d \geq 0.003m_p$ will be reflected in the first gap of the reflectron. Parent ions show a

(10) Grimsrud, E. P.; Kebarle, P. *J. Am. Chem. Soc.* **1973**, *95*, 7939.
(11) Morgan, S.; Keesee, R. G.; Castleman, A. W., Jr. The Relation of Cluster Dissociation, Magic Numbers, and Thermodynamic Stabilities: Consideration of Ammonia Clusters Studied Via Multiphoton Ionization, to be submitted.
(12) Morgan, S.; Castleman, A. W., Jr. Dissociation Dynamics of Methanol Clusters Following Multiphoton Ionization *J. Phys. Chem.*, in press.
(13) Stace, A. J.; Shukla, A. K. *J. Am. Chem. Soc.* **1982**, *104*, 5314.
(14) Nishi, N.; Kamamoto, Y. *J. Am. Chem. Soc.* **1987**, *109*, 7353.

smooth decrease in intensity from $H^+(CH_3OH)_2$ and beyond. Daughter ions formed from unimolecular decay and collision-induced dissociation precede the parent ions by approximately 0.6 μs. The daughter ion intensity peaks at $n = 7$. Many peaks arising from hydrocarbon impurities $C_xH_y^+$ (from the background pump oil) are observed at arrival times under 16 μs. CH_3O^+ and $H^+(CH_3OH)$ are also observed in this region (immediately preceding 16 μs). Peaks representing mixed clusters of form $H^+(H_2O)(CH_3OH)_n$, labeled **b**, are observed for $n = 6$ to $n = 11$; at larger n their peaks overlap those of the protonated methanol ions (parent ions, sequence **a**).

Daughter ions are easily identified in Figure 5 under conditions where parent ions are excluded from the spectrum; this is accomplished by reducing the potential U_K below U_T. The TOF of the daughter ions remains constant because they are reflected between the first two grids of the reflectron. The window for observing dissociation in the drift region encompasses the field-free region from the last (ground) grid of the TOF ion lens to the reflectron entrance, i.e., a distance of 41 cm. This represents a time window of about $0.1\sqrt{m_p} \leq t \leq 0.9\sqrt{m_p}$ (m_p is the mass in amu of the parent ion, and t is in microseconds), when the electric fields in gaps 1 and 2 of the TOF ion lens are, respectively, 300 and 950 V/cm, and the parent ion birth potential is 1164 V.

Five types of peaks (labeled **d**–**h**) are seen clearly in the spectrum. Peaks labeled **d** correspond to a mass loss of 32 amu from a parent ion cluster that enters the drift region as $H^+(CH_3OH)_n$ (these are analogous to the **a** peaks in Figure 2) as shown below:

$$H^+(CH_3OH)_n \rightarrow H^+(CH_3OH)_{n-1} + CH_3OH \quad (4)$$

The unimolecular and collision-induced processes which are responsible for the above decay reaction are discussed elsewhere.[12] Mass losses of more than one monomer unit, not readily apparent in Figure 5, are observed when the potential at grid T is lowered to slightly above the cutoff voltage for the $n - i$ daughter ion resulting in increased mass resolution.

$$H^+(CH_3OH)_n \rightarrow H^+(CH_3OH)_{n-i} + iCH_3OH \quad (5)$$

These multiple monomer unit losses appear as unresolved shoulders on the early arrival side of the **d** peaks in Figure 5. The loss of up to five methanol monomers from the protonated octamer is observed.[12]

The peak designated **e** in Figure 5 corresponds to loss of water from the protonated methanol dimer ion,

$$H^+(CH_3OH)_2 \rightarrow (CH_3)_2OH^+ + H_2O \quad (6)$$

a process requiring an induction time of at least several tenths of a microsecond; the mechanism is discussed in detail in a previous publication.[9]

The reflected ions which do not dissociate in the field-free region account for the peaks labeled **f**. Fragmentation of larger ions into smaller ion mass channels in the ion lens causes asymmetric parent ion peaks.[15] The asymmetric tail section of these peaks is composed of lower energy ions born at a lower potential than the ions born in the laser interaction region. In Figure 5 the potential at grid T is slightly above that of these low energy ions, labeled **f**, hence resulting in their reflection and inclusion in the mass spectrum.

Of particular interest are the peaks labeled **g** and h. Their existence provides additional evidence favoring mechanism I for the formation of mixed cluster ions. Peaks labeled h correspond to loss of 78 amu from $H^+(CH_3OH)_n$, indicating loss of both a methanol monomer and C_2H_6O (dimethyl ether) for parent ions $n = 4$ through 9 in the drift region. Peaks designated as **g** in Figure 5 represent the loss of one methanol moiety from the mixed cluster species $H^+(H_2O)(CH_3OH)_n$ (peaks labeled **b** in Figures 2 and 4); as clearly seen in Figure 4 this sequence begins at 32 μs ($n = 6$) and continues for all parent mixed cluster sizes corresponding to arrival times out to 50 μs. If these clusters are also formed by reaction 2, they initially contained nine or more methanol molecules. It is observed that the protonated methanol dimer ion eliminates H_2O while retaining dimethyl ether as described by reaction 6. Analogous water elimination reactions are not observed for the parent cluster ions larger than $n = 2$.

(15) Kuhlewind, H.; Neusser, H. J.; Schlag, E. W. *Int. J. Mass Spectrom. Ion Phys.* **1983**, *51*, 255.

Table I. Dissociation Reactions of Methanol Clusters Following Multiphoton Ionization

dissociation reaction	figure	peaks	observed domain
$[(CH_3OH)_n^+]^* \rightarrow H^+(CH_3OH)_{n-1} + CH_3O$	2	a	ion lens
$[H^+(CH_3OH)_2]^* \rightarrow (CH_3)_2OH^+ + H_2O$	5	e	drift region
$[H^+(CH_3OH)_n]^* \rightarrow H^+(CH_3OH)_{n-i} + iCH_3OH$	5	d ($i = 1$)	drift region
$[H^+(CH_3OH)_n]^* \rightarrow H^+(H_2O)(CH_3OH)_{n-3} + (CH_3)_2O + CH_3OH$	2 5	b h	ion lens drift region
$[H^+(H_2O)(CH_3OH)_n]^* \rightarrow H^+(H_2O)(CH_3OH)_{n-1} + CH_3OH$	5	g	drift region

In the case of these larger clusters, H_3O^+ is solvated more strongly by methanol than is protonated dimethyl ether, $(CH_3)_2OH^+$.[8] Hence for these clusters water retention and dimethyl ether elimination lead to production of mixed clusters of form $H^+(H_2O)(CH_3OH)_n$. Prompt (immediately following ionization) loss of dimethyl ether in the TOF ion lens, as proposed in mechanism I, results in the mixed cluster sequence labeled **b** in Figure 2, the conventional time-of-flight mass spectrum. These mixed clusters formed by rapid decay processes in the ion lens subsequently dissociate in the field-free region via loss of one methanol monomer to form the sequence **g** peaks in Figure 5. In contrast, a "slower" elimination of dimethyl ether in the drift region (along with CH_3OH) from cluster sizes $H^+(CH_3OH)_n$, $n = 4$ through 9, results in the peak sequence labeled **h** in Figure 5. Thus, a signficant difference in reactivity with cluster size is observed; the smaller clusters lose dimethyl ether on a longer (field-free region) time scale while the larger clusters undergo comparatively rapid loss of C_2H_6O in the ion lens. The overlap of the **g** and h distributions in Figure 5 indicates that, for a certain range of initially formed cluster sizes, the dissociation process spans both time scales. However, it is observed that as the peaks labeled h (representing dissociation in the field-free region) diminish in intensity, those peaks labeled **g** (indicating dissociation in the acceleration field) increase. The overlap of these two distributions points to mechanism I as the mixed cluster production method. Additionally, the peaks labeled h cannot be derived from neutral clusters containing water. The reflectron experiments demonstrate that these peaks evolve from protonated methanol clusters. A summary of all observed reactions of the methanol clusters is presented in Table I.

Discussion and Conclusions

The predominant unimolecular reactions involving loss of one or more monomer units exhibit no specificity with cluster size, and the "splitting off" of monomer units and multiples thereof from the clusters occurs for all sizes studied. In a cluster composed of such units there are always a number of "surface" monomer unit entities that can be relatively easily dissociated.

In contrast, however, reactions of methanol clusters presented in Table I, together with mass spectra displayed in Figures 2, 4, and 5, and results from previous publicatons,[9] reveal a distinct dependence on degree of solvaton for certain reactions of methanol clusters following multiphoton ionization. It is also not surprising that reactions requiring extensive rearrangement (the ion–molecule reactions) proceed only for cluster sizes where this rearrangement is presumably facile. The first such incidence investigated by us in the methanol system involves the previously reported[9] loss of water from the protonated methanol dimer ion $H^+(CH_3OH)_2$. The reaction is specific to only the aforementioned cluster size.

Using available thermochemical data,[8] we have made rough estimates of the energetics for competitive loss processes from the protonated methanol trimer, including rearrangement reactions that would lead to different ion cores. The values suggest that several channels corresponding to dehydrogenation reactions and rearranged ion cores are possible for the protonated trimer. Hence,

it is concluded that failure to observe these must be due to the necessity of substantial molecular rearrangement to facilitate the formation of an H_2O bound in an appropriate configuration for loss. Evidently energy dissipation through CH_3OH loss is much more facile and is the dominant channel at intermediate cluster sizes; in fact, it is the only channel observed for the protonated trimer.

In addition to the evaporative loss of methanol, and the reaction of the protonated dimer which leads to the production of protonated dimethyl ether and elimination of water, several other size-dependent intracluster reaction pathways have been revealed in the present study. In the case of intermediate and larger clusters, $(CH_3)_2O$ (along with CH_3OH) is lost while H_2O is retained by the cluster. For clusters comprised of four to nine methanol molecules, the $(CH_3)_2O$ elimination is observed to occur over the time window 1 to 15 μs after ionization as evidenced by the observed mass loss during flight through the field-free region to the reflectron.

For larger clusters, the appearance of $H^+(H_2O)(CH_3OH)_n$ in the conventional TOF mass spectrum implies that the elimination takes place well before the ions enter the field-free region. The loss of $(CH_3)_2O$ occurs on a rapid time scale (in the ion lens) creating mixed clusters of form $H^+{\cdot}H_2O(CH_3OH)_n$ where n = 7 or greater (**b** peaks, Figure 2). An ion with the mass of $H^+(CH_3OH)_7$ requires about 1.3 μs to exit the acceleration field and enter the field-free region under the experimental conditions employed in the experiments.

The results can be explained by estimates that ether is only slightly more strongly bound than methanol to protonated methanol clusters of size n = 4, and the solvation may be about thermoneutral at n = 5. Beyond this size the solvation of CH_3OH may be preferential. The reason why $(CH_3)_2O$ elimination is accompanied by CH_3OH loss is not clear. It may be that the excess energy of the rearrangement is accommodated through evaporative methanol loss.

Based on high-pressure mass spectrometric measurements of mixed protonated alcohol–water clusters comprised of all combinations up to a total of six molecules, Kebarle and co-workers[10] concluded that in small ion clusters methanol is preferentially solvated by the proton, while in ones with more than a total of nine molecules, interaction with water would dominate over that of methanol. It is worth noting that these findings are in general accord with the results of Stace and Shukla[13] who present fragmentation results for mixed water–methanol cluster studies which display a reversal in the trend of water and methanol loss with cluster size from preformed mixed cluster systems. In view of an expected switch-over in relative solvation, our findings of the appearance of a protonated water cluster bound with methanol molecules beginning at size n = 7 is consistent with these findings.

Acknowledgment. Financial support by the U.S. Department of Energy, Grant DE-ACO2-82ER60055, is gratefully acknowledged and the Army Research Office, Grant No. DAAG29-85-K0215.

Registry No. CH_3OH, 67-56-1.

Periodic Trends in Chemical Reactivity: Reactions of Sc^+, Y^+, La^+, and Lu^+ with Methane and Ethane

L. S. Sunderlin[†] and P. B. Armentrout*[,‡,§]

Contribution from the Departments of Chemistry, University of California, Berkeley, California 94720, and University of Utah, Salt Lake City, Utah 84112.
Received September 19, 1988

Abstract: The reactions of Sc^+, Y^+, La^+, and Lu^+ with methane and ethane are examined using guided ion beam mass spectrometry. With methane, the major products are MCH_2^+ at low energy and MH^+ at high energy, with small amounts of MCH_3^+ also seen. The results for reaction of Y^+, La^+, and Lu^+ with ethane are similar to those reported previously for Sc^+. Single and double dehydrogenation are exothermic for Sc^+, Y^+, and La^+ but endothermic for Lu^+. MH_2^+ is formed in endothermic reactions at low energies for all four metals. At high energy, MH^+, MCH_2^+, and MCH_3^+ are the major products. A molecular orbital model previously used to explain the reactivity of metal ions with H_2 is extended to explain the reactivity seen here. The results are analyzed to give $D°(M^+–CH_2)$, $D°(M^+–CH_3)$, the two-ligand bond energy of $D°(M^+–H) + D°(HM^+–H)$, and limits on $D°(M^+–C_2H_4)$ and $D°(M^+–C_2H_2)$ for all four metals.

Extensive progress in understanding the gas-phase activation of carbon–hydrogen and carbon–carbon bonds by transition-metal ions has been made recently.[1,2] Such studies can provide quantitative thermochemistry[3] as well as insight into the periodic trends of reactivity.[1,4] Recent studies in our laboratories have shown that the reactions of atomic transition-metal ions with dihydrogen are sensitive to the electronic state and configuration of the metal ion and have formulated guidelines describing the reactivity seen.[4,5] A previous paper that covers the reaction of H_2 with Sc^+ and its isovalent analogues, Y^+, La^+, and Lu^+, completes the study of the first row of the transition metals and compares reactivity trends within a column of the periodic table.[6] The reactivity guidelines derived in the H_2 system have also been extended to the reactions of Ti^+,[7] V^+,[8] Cr^+,[9] and Fe^+[10] with methane. This paper is a continuation of our investigations of the periodic trends in the reactivity of transition-metal ions with

[†] University of California.
[‡] University of Utah.
[§] NSF Presidential Young Investigator 1984–1989; Alfred P. Sloan Fellow; Camille and Henry Dreyfus Teacher-Scholar, 1988–1993.

(1) Armentrout, P. B. *Gas Phase Inorganic Chemistry*. In Modern Inorganic Chemistry; Russell, D. H., Ed.; Plenum: New York, 1989.
(2) Allison, J. *Prog. Inorg. Chem.* **1986**, *34*, 627–676, and references therein.
(3) Armentrout, P. B.; Georgiadis, R. *Polyhedron* **1988**, *7*, 1573–1581.
(4) Elkind, J. L., Armentrout, P. B. *J. Phys. Chem.* **1987**, *91*, 2037–2045.
(5) Elkind, J. L.; Armentrout, P. B. *J. Phys. Chem.* **1985**, *89*, 5626–5636; **1986**, *90*, 5736–5745, 6576–6586; *J. Chem. Phys.* **1986**, *84*, 4862–4871; **1987**, *86*, 1868–1877; *Int. J. Mass Spectrom. Ion Processes* **1988**, *83*, 259–284.
(6) Elkind, J. L.; Sunderlin, L. S.; Armentrout, P. B. *J. Phys. Chem.*, in press.
(7) Sunderlin, L. S.; Armentrout, P. B. *J. Phys. Chem.* **1988**, *92*, 1209–1219.
(8) Aristov, N.; Armentrout, P. B. *J. Phys. Chem.* **1987**, *91*, 6178–6188.
(9) Georgiadis, R.; Armentrout, P. B. *J. Phys. Chem.* **1988**, *92*, 7060–7067.
(10) Schultz, R. H.; Elkind, J. L.; Armentrout, P. B. *J. Am. Chem. Soc.* **1988**, *110*, 411–423.

0002-7863/89/1511-3845$01.50/0